THERMO-LUMINESCENCE PROPERTIES OF Ce^{3+} & Dy^{3+} DOPED DICALCIUM MAGNESIUM DISILICATE, $Ca_2MgSi_2O_7$

DIPTI PANDEY

School of Studies in Physics and Astrophysics, Pt. Ravishankar Shukla University, Raipur (C.G.), India

AND

DR. NAMEETA BRAHME, DR. RAVI SHARMA

Department of Physics, Govt. Arts and Commerce Girls College, Devandra Nagar, Raipur (C.G.), India

A long after glow phosphor $Ca_2MgSi_2O_7$: Ce^{3+}, Dy^{3+} were prepared by solid state reaction method under a weak reducing atmosphere. The prepared phosphor was characterized by *X* ray diffraction (XRD), Scanning electron microscope (SEM), EDX, thermo luminescence (TL) properties of dicalcium magnesium disilicate $Ca_2MgSi_2O_7$ doped with different rare earth ions and with different concentration were investigated. Also the effect of Ce^{3+} & Dy^{3+} concentration at fixed UV exposure time was studied. The TL intensity was recorded for different exposure time with UV light (λ = 254 nm) and it was observed that TL intensity is maximum for 5 min exposure time for Ce^{3+} & 10 min exposure time for Dy^{3+}. It is also observed that $Ca_2MgSi_2O_7$ doped with cerium is a good dopant as compared to other dopants and dopant concentration of 0.4 mol % cerium gives maximum TL emission. The activation energy and frequency factors of trap centres of the $Ca_2MgSi_2O_7$: Ce, Dy were calculated by thermoluminescence curve. Thermo luminescence curve indicated that the trap centres were more helpful to the long lasting phosphorescnce. For $Ca_2MgSi_2O_7$: Ce^{3+} with thermal depth of trap or activation energy 0.27 eV. The well defined 293.87°C can be advantageously used for high temperature dosimetry applications.

KEYWORDS : Dicalcium magnesium disilicate, SEM, XRD, EDX, thermoluminescence, radiation dosimetry.

INTRODUCTION

The luminescence is normally generated by luminescent centers, namely activators, incorporated on specific lattice sites in crystalline hosts. The activators are mostly rare earth ions or transition metal ions, such as europium, cerium, dysprosium, etc. Covering a wide materials range, typical examples of host lattices include sulfides, oxides, aluminates, silicates, phosphate, borates, etc. Silicates based phosphors are efficient luminescent materials, mainly because of their rigid and much better characteristics , such as brighter luminescence , a longer duration of time of the phosphorescence, along with easier preparation and low cost. Several silicate materials doped with rare earth (Rn^+) ions, either divalent or trivalent, have been

proposed for or used as commercial phosphors in tricolor fluorescent lamps, scintillators . Despite their excellent host matrix properties, the silicates are not completely free of lattice defects which may decrease drastically the luminescent efficiency or cause undesired properties *e.g.* afterglow as is the case with the Ce^{3+} doped rare earth oxyorthosilicates (R_2SiO_5 : Ce^{3+} R = Y, Lu) [2, 3]. Trivalent cerium Ce^{3+} has been widely applied in the phosphor materials for phosphor converted white light emitting diode as an activator ion. Because the Ce^{3+} activated phosphors show the strong broad excitation and emission band due to the spin allowed energy transitions between the $4f$ ground state and 5d excited state of Ce^{3+} . $M_2MgSi_2O_7$ (Sr, Ca) doped with Eu^{2+} and Dy^{3+} phosphor has shown quite good long lasting behaviour. Silicate phosphors have few advantages over previously developed aluminate long lasting phosphors on chemical stability, heat stability, lower cost and varied luminescence colour from blue to yellow [10]. The experimental result indicated that Ce^{3+} ions could not be only trap centre but also act as luminescence centre [9].
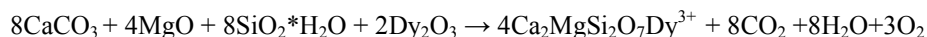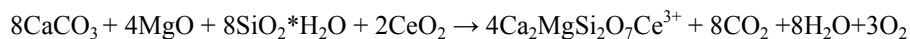
The thermoluminescence phenomenon occurs when the semiconductor material is exposed to ionizing radiation. A fraction of free electrons or holes are produced due to the exposure or radiation and they may be trapped by defects named as traps present within the crystal lattice of the prepared phosphor materials. If the traps are deep enough means the requirement of energy is too higher, the trapped charges may remain in those sites for an extended period of time. As the material is heated by external source, the trapped charges may escape from the trapping centers and then recombine with other trapped charges with opposite sign. The emission of light, so called thermoluminescent-signal occurs during the recombination process. Although many natural minerals are thermoluminescent, the most efficient TL materials are almost always formulated synthetic materials.

In this paper, we present a detailed study about the luminescence properties of the dicalcium magnesium disilicates ($Ca_2MgSi_2O_7$) doped with Ce^{3+}, Dy^{3+} phosphors which were prepared by a solid state reaction. The preparation and crystal structure were studied by thermal analysis and X-ray powder diffraction, respectively. The thermo-luminescence properties were investigated, too. In this work, we also explained that cerium ion Ce^{3+} to enhance the long persistent afterglow in $Ca_2MgSi_2O_7$ phosphor. However in Ce^{3+} is found most suitable for enhancing the luminescent properties. The main objective of this paper that the Ce^{3+} rare earth ion doped $Ca_2MgSi_2O_7$ phosphor is good for high temperature dosimetric application.

EXPERIMENTAL

Solid state synthesis of samples

$Ca_2MgSi_2O_7$: Ce was prepared by solid state reaction method. $CaCO_3$, SiO_2, MgO and CeO_2, Dy_2O_3 were used as raw materials. The nominal Ce, and DY molar concentration relative to the host compound were chosen. The mixture of raw materials was ground to fine particle before sintering for $3h$ in air at 1200°C for $Ca_2MgSi_2O_7$: RE (RE = Ce, Dy) preparation. Thus the prepared sample is white powder. The chemical reaction used for stoichiometric calculation is

$8CaCO_3 + 4MgO + 8SiO_2*H_2O + 2CeO_2 \rightarrow 4Ca_2MgSi_2O_7Ce^{3+} + 8CO_2 + 8H_2O + 3O_2$

$8CaCO_3 + 4MgO + 8SiO_2*H_2O + 2Dy_2O_3 \rightarrow 4Ca_2MgSi_2O_7Dy^{3+} + 8CO_2 + 8H_2O + 3O_2$

CaMg-a° kermanite

The reaction process involves the decomposition of $CaCO_3$ when the temperature is higher than about 900°C according to

$$CaCO_3 \rightarrow CaO + CO_2 \ (\ T \geq 900^0C)$$
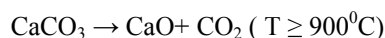
Characterization of prepared sample

The crystalline structure of the sample was verified by *X* ray powder diffraction (XRD) . The XRD measurement were carried out using Bruker D8 advanced *X*-ray powder diffractometer . The *x* rays were produced using a sealed tube & the wavelength of the *X*-rays was 0.154 nm (Cu K-alpha). The thermoluminescence studies were carried out using TLD reader I1009 supplied by Nucleonix Sys. Pvt. Ltd.. The sample was irradiated by UV radiation 254 nm. The heating rate used for TL measurement is 6.7° C/s. Kinetic parameter evaluated by initial rise method and graph plotted by Origin 6.1.

RESULTS AND DISCUSSION

3.1. XRD analysis result

The mean size of particles is a very important variable for the brightness and processing of phosphor materials. Fig .1 shows XRD patterns of prepared samples with a, Ce^{3+}, Dy^{3+} doping concentration of 4%. It is observed that the crystal structure has a tetragonal symmetry with a space group $P42_1m$. No impurity phase has been observed in any of the samples, clearly implying that the obtained samples are single phase and doped Dy^{3+} do not cause any significant change in the host structure. The crystalline sizes (*D*) and strain of various samples are estimated using Scherrer'sformula and FWHM method. According to which $D = K\lambda/\beta \cos \theta$ and strain $\varepsilon = \lambda/\sin \theta \ [\beta \cos \theta/\lambda – K/D]$ where *K* is the Scherrer's constant, λ-the *X*-ray wavelength of Cu-Kα radiations (1·54 Å), β-the peak width of half-maximum (FWHM) and θ is the Bragg′s diffraction angle. The calculated average crystallite Size is about 67 nm. The corresponding XRD data for indexed are summarized in table 1, 2. In table 3 Where K (= 0.9) is crystalline shape constant and other parameters have the same meaning as in eqn. 1. The strain ε is estimated from the slope of the line and the crystalline size. The strain of as prepared sample are found to be – 0.22, – 0.23 with 0.4% Ce^{3+}, Dy^{3+} concentration respectively. Here negative sign indicates compressive strain in $Ca_2MgSi_2O_7 : Dy^{3+}$ and $Ca_2MgSi_2O_7: Ce^{3+}$.

Table 1. Details of XRD data of nanocrystalline $Ca_2MgSi_2O_7 : Dy^{3+}$ 0.4 mol % phosphors

2θ (dgree)	θ (dgree)	Sin θ (degree)	I (a.u)	d (A°)
23.28	11.64	0.2017617	166	7.63
24.02	12.01	0.208082	190	7.40
25.48	12.74	0.2205227	206	6.98
27.06	13.53	0.2339544	182	6.58
29.06	14.53	0.2508869	274	6.14
30.14	15.07	0.259998	308	5.92
31.24	15.62	0.26925601	765	5.72
36.36	18.18	0.312003	167.8	4.94
45.54	22.77	0.3870328	170	3.98
51.92	25.96	0.437744	136	3.45

Table 2. Details of XRD data of nanocrystalline $Ca_2MgSi_2O_7 : Ce^{3+}$ 0.4 mol % phosphors

2θ (degree)	θ (degree)	$Sin\theta$ (degree)	I (a.u)	d (A°)
21.88	10.94	0.1898	292.9	8.11
26.6	13.3	0.230	629.2	6.69
28.56	14.28	0.247	614	6.24
31.14	15.57	0.268	651.4	5.75
33.4	16.7	0.287	892	5.37
40.72	20.36	0.348	238	4.43
42.92	21.46	0.366	222.5	4.21
47.56	23.78	0.403	419.9	3.82
47.52	23.76	0.403	183.7	3.82
56.32	28.16	0.472	200.3	3.26
60.38	30.19	0.503	159.7	3.06

Table 3. The comparison of particle sizes band gaps and strain of $Ca_2MgSi_2O_7$ with different dopants (Ce^{3+}, Dy^{3+}, Eu^{2+}) for 0.4 mol %

Composition	Size by crystalline	Band Gap	Strain
$Ca_2MgSi_2O_7;Ce^{3+}$	19.69	5.2	0.22
$Ca_2MgSi_2O_7;Dy^{3+}$	19.58	5.1	0.23
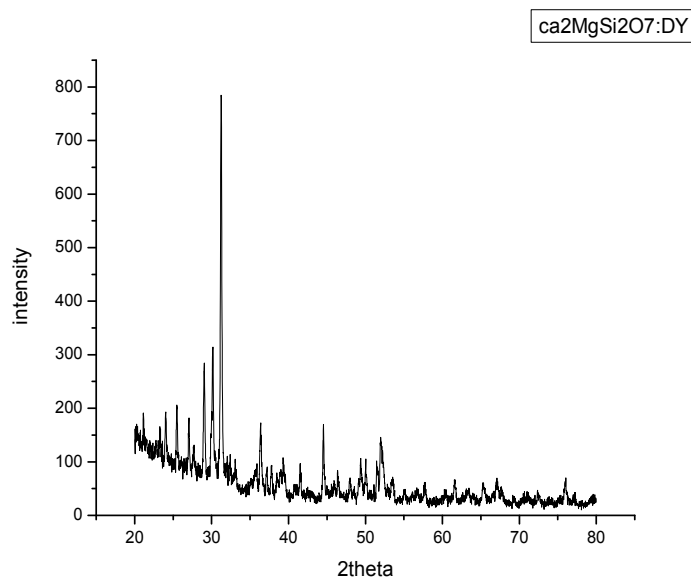
Fig : XRD pattern of $Ca_2MgSi_2O_7 :Dy^{3+}$ phosphor.
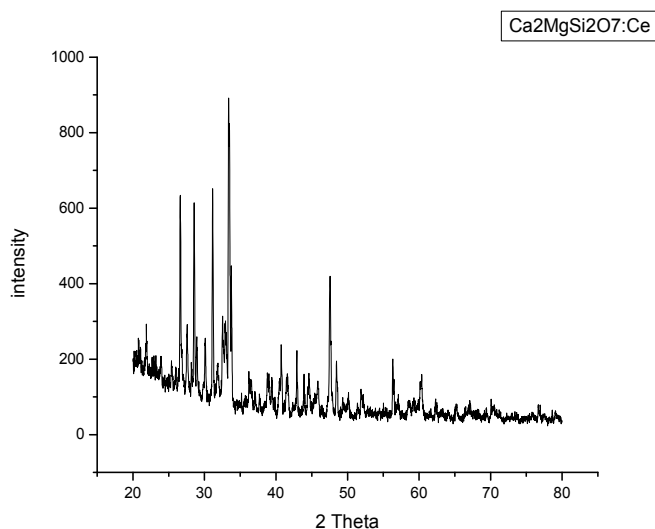
Ca2MgSi2O7:Ce

Fig: : XRD pattern of Ca$_2$MgSi$_2$O$_7$:Ce^{3+} phosphor.

3.2. Scanning Electron Microscopy (SEM)

The morphology of materials was determined by high resolutions microscope. Here the morphology and size of the prepared materials were determined from SEM studies. Fig. 2 (a) and (b) full view of SEM image and partial view of SEM images of the typical surface morphologies of the ground phosphors synthesized by solid state reaction method. In this image it can be observed that the prepared sample consists of the particle size distribution 1mm and 500 nm.
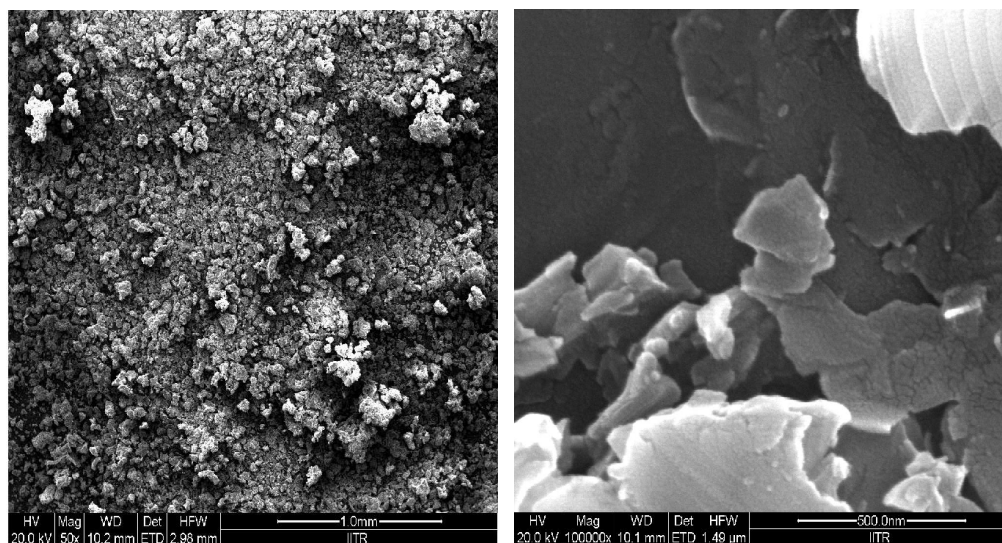

Fig. 2(a) : SEM photographs of Ca$_2$MgSi$_2$O$_7$: Dy^{3+} 0.4 mol % particles prepared by solid state reaction method.
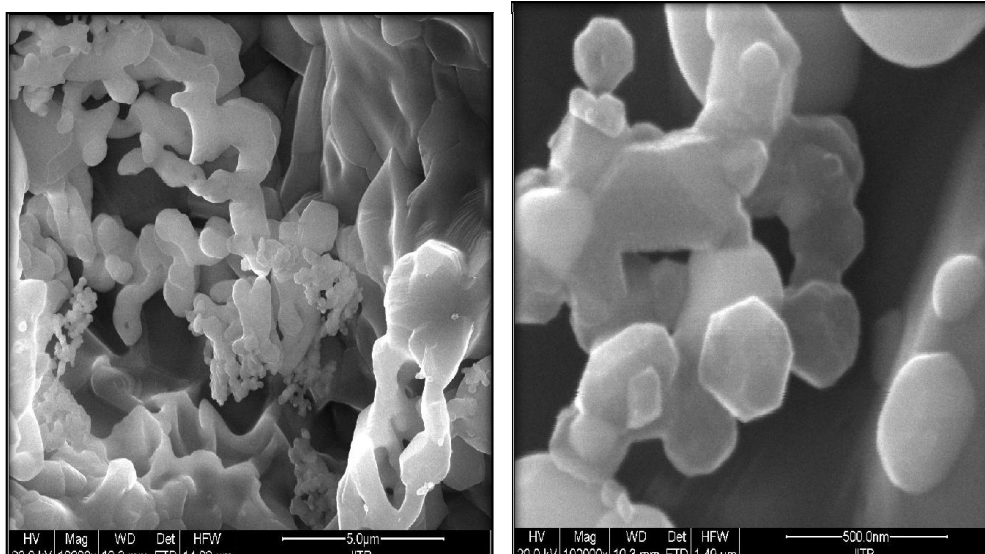
Fig (b): SEM photographs of Ca$_2$MgSi$_2$O$_7$: Ce^{3+}0.4 mol% particles prepared by solid state reaction method.

Thermo luminescence studies of Ca$_2$MgSi$_2$O$_7$: RE (RE = Ce, Dy)

Thermo-luminescence is a useful tool is investigating the properties of the traps responsible for the afterglow. The thermo-luminescence (TL) glow curves of the prepared sample Ca$_2$MgSi$_2$O$_7$ doped with Ce^{3+}, DY^{3+} after UV irradiation were recorded. The TL glow curves for different Ce^{3+}, Dy^{3+} concentration and different UV doses at a heating rate of 6.7°CS^{-1} are shown below. For clearity and comparison, only the thermo-luminescence curves of the different dopants Dy^{3+}, Ce^{3+} (0.1 mol %, 0.2 mol %, 0.4 mol %, 0.5 mol %) concentration are presented in fig. 3. Fig. 3 (a) shows that , the thermo-luminescence curve of Ce^{3+} recorded exhibit rich structure and substantial intensity in the range from 50°C to 375°C.The TL glow curve of Ce^{3+} doped Ca$_2$MgSi$_2$O$_7$ phosphor has two glow peaks. For the variable concentration of Ce^{3+} (0.1 mol % to 0.5 mol %) shows major TL peak at 293.87°C and the minor peak is at 108.13°C. The TL glow curve of Ca$_2$MgSi$_2$O$_7$: Dy^{3+} for variable concentration (0.1 mol% to 0.5 mol %) shown in fig. (b). The TL glow curve of 0.1 mol % Dy^{3+} doped Ca$_2$MgSi$_2$O$_7$ phosphor gives no TL emission. Ca$_2$MgSi$_2$O$_7$: Dy^{3+} (0.2 mol %, 0.4 mol % 0.5 mol 5) shows a sharp intense peak around at 95°C with a minor peak around at 290°C. It is also observed that 0.4 mol % & 0.5 mol % Dy$^+$ doped phosphors shows two TL glow peaked were both separated from TL glow curve and represented as curve in fig. 3(b). In all three curves , it is observed that There is no significant change in peak position ,it is fixed with variable concentration of *RE* (= Ce^{3+}, Dy^{3+}) only TL intensity increases with increasing the concentration of dopant up to 0.4 mol % after that the relative TL intensity decrease due to concentration quenching occurs. It is also observed that TL intensity of Ce^{3+}doped phosphor is maximum compared to Dy^{3+} doped phosphors. The sensitivity of Ce^{3+} doped phosphor is nearly very twice as that of Dy^{3+} ones. It is important to notice that using the right dopant concentration, it is possible to maximize the TL efficiency and improve sensitivity and dose linearity for a specific irradiation type [8]. The peak observed at 95^{0}C for Dy^{3+} doped one is not suitable for dosimetry application as its fading rate will be very high. The major peak at 293.87^{0}C in case of Ce^{3+}doped phosphor can be used for dosimerty application. It is seen that 0.4 mol % of Ce concentration gives maximum TL emission in table.
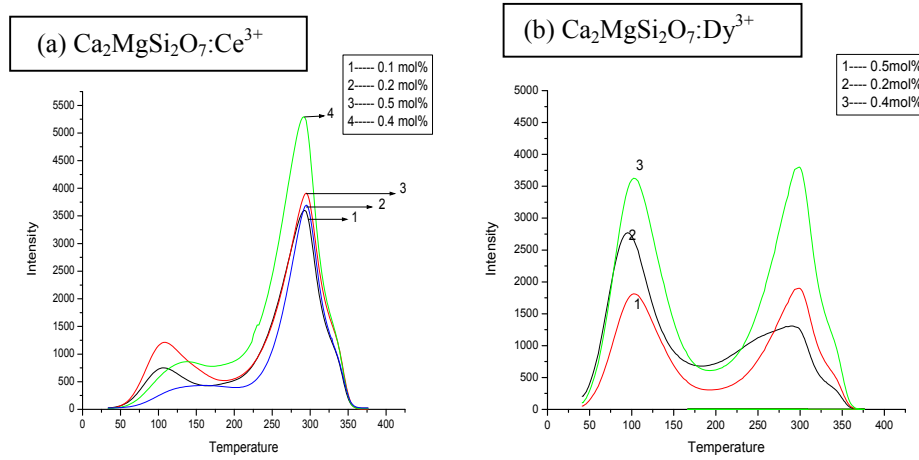
Fig 3 (a) TL glow curve Ca₂MgSi₂O₇ : Ce³⁺ for 5min UV exposure time with heating at 6.7°C/S.
(b) TL glow curve of Ca₂MgSi₂O₇ : Dy³⁺ for10 min UV exposure time with heating rate 6.7°C/S.
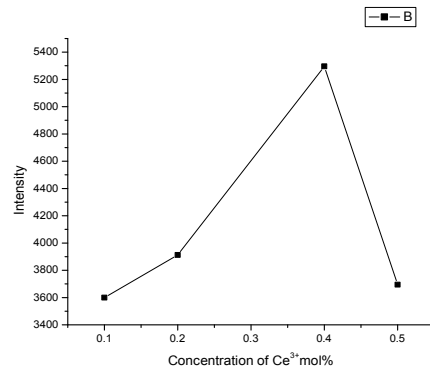
Fig. 4(a). TL glow curve intensities of Ca₂MgSi₂O₇ : Ce³⁺ for 5 min UV exposure time with heating rate at 6.7°C/S.
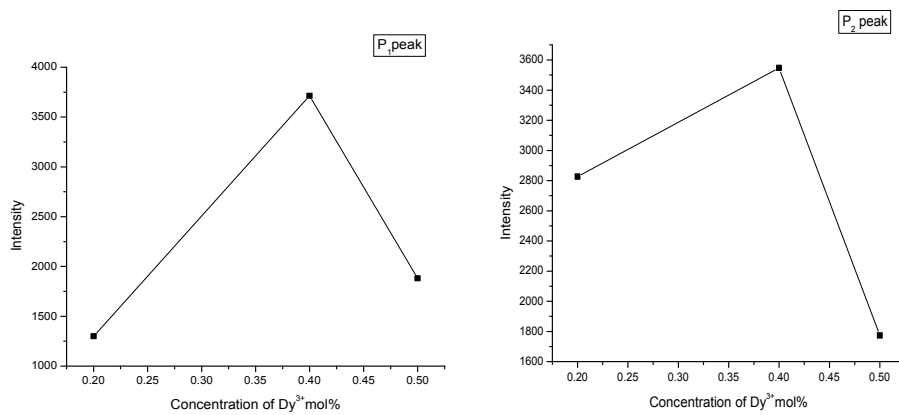
(b) The first Peak of TL glow curve intensities of Ca₂MgSi₂O₇ : Dy³⁺ for 10min UV exposure time with heating rate at 6.7°C/S.
(b') The second peak of TL glow curve intensities of Ca₂MgSi₂O₇ : Dy³⁺ for 10 min UV exposure time with heating rate at 6.7°C

Table 3 (a). Comparison of TL response of Ce^{3+} doped phosphor.

Composition	Maximum TL intensity peak temp		Relative TL intensity	
	First peak	Second peak	First peak	Second peak
0.1 mol% Ce^{3+}	98.27°C	293.87°C	751.37	3600
0.2 mol% Ce^{3+}	98.71°C	293.87°C	1151.91	3911.87
0. 4 mol% Ce^{3+}	133.1°C	293.87°C	862.29	5295.72
0.5 mol% Ce^{3+}	128.27°C	293.87°C	400.28	3694.52

Table 3(b) : Comparison of TL response of Dy^{3+} doped phosphor.

Composition	Maximum TL intensity peak temp		Relative TL intensity	
	First peak	Second peak	First peak	Second peak
0.2 mol% Dy^{3+}	95°C	293.1°C	1299	2826.85
0. 4 mol% Dy^{3+}	95°C	293.1°C	3713.6	3547.2
0.5 mol% Dy^{3+}	95°C	293.1°C	1881.675	1773.6

Effect of UV exposure time on TL intensity of Ca$_2$MgSi$_2$O$_7$: RE (RE = Ce^{3+}, Dy^{3+}) and calculation of kinetic parameters

Fig. 5 (a) and (b) shows TL glow curves for optimized concentration of RE (= Ce^{3+}) 0.4 mol% with different UV radiation times such as 1min , 3min, 5min and 7min for Ce^{3+} and TL glow curve of Dy^{3+} dopant with different UV radiation times such as 5 min,10 min, 20 min & 25 min. It is observed that TL intensity is gradually increases with increasing the UV exposure time and optimized UV exposure time is 5min for Ce^{3+} where maximum TL glow intensity was found. Similarly we were obtained the TL glow curve in Dy^{3+} dopant but optimized UV exposure time for 10 min where maximum TL glow intensity was found. The calculation of kinetic parameters (activation energy in e V and frequency factor in S^{-1}) was determined by various method such as peak shape method , initial rise method and fitting rise method. In fig 5(a) & (b) , all major peaks shows the first order kinetics because the value of shape factor $\mu = T_2 - T_M /T_2 - T_\mathrm{L} \approx 0.42$ or less than 0.42 shows first order kinetic glow curve. The minor peaks shows the second order kinetic (0.55). So the nature of dual peak concern it is very difficult to determine the kinetic parameters of dual nature of peak than we compare the kinetic parameter calculated by peak shape method. Initial rise method valid for both of kinetics is based on the fact that the TL intensity of the as cending part of the curve and temperature is related to each other by the relation I_{TL} α exp (– *Et/kT*) [11]. Therefore, E_t values can be obtained from the slope of the Arrhenius plot ln (I_{TL}) vs. $1/T$ as seen in fig. For the variation of dopant Ce^{3+} the activation energies   and relative frequency factor shows in table. The trap depth and frequency factor were calculated using initial rise method come out to be in between 0.27 e V to .31 e V & 0.17 e V to 0.43 e V for optimized concentration of Ce^{3+} & Dy^{3+} rare earth doped phosphors and relative frequency factor are in the range 0.19 to 1.13 × 10^8 H$_Z$ & 1.63 to 1.67 × 10^8 H$_Z$.

Table 4 (a): Trap parameters of corresponding major TL glow peak of Ca$_2$MgSi$_2$O$_7$: Ce^{3+} with different concentration for optimized UV exposure time.

Ce^{3+} concentration	Peak	Activation energy	Frequency factor
0.1 mol%	P$_1$+P$_2$	0.28 e V	0.19 × 10^8
0.2 mol%	P$_1$+P$_2$	0.31 e V	0.42 × 10^8
0.4 mol%	P$_1$+P$_2$	0.27 e V	1.13 × 10^8
0.5 mol%	P$_1$+P$_2$	0.28e V	0.35 ×10^8

Table 4 (b) : Trap parameters of corresponding major TL glow peak of
$Ca_2MgSi_2O_7 : Dy^{3+}$ with different concentration for optimized UV exposure time

Dy^{3+} concentration	Peak	Activation energy	Frequency factor
0.2 mol%	$P_1 + P_2$	0.17 e V	1.63 S^{-1}
0.4 mol%	$P_1 + P_2$	0.43 e V	1.67 S^{-1}
0.5 mol%	$P_1 + P_2$	0.17e V	1.63 S^{-1}

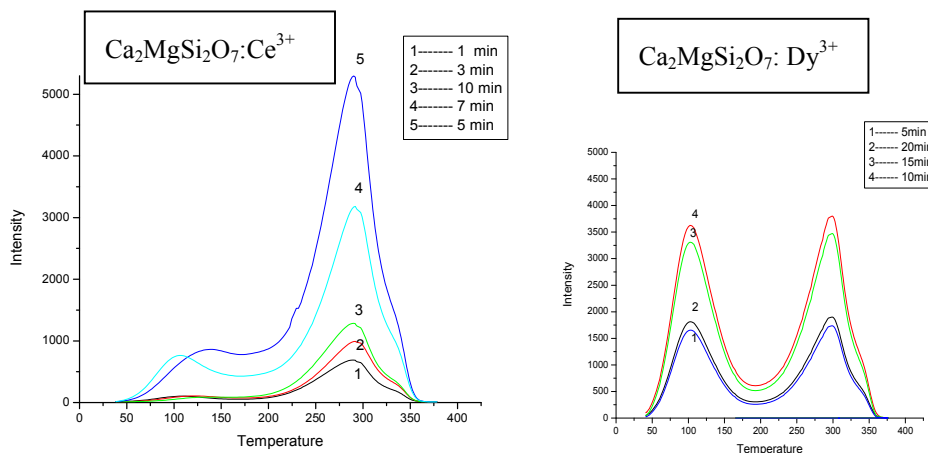**Fig 5 (a) TL glow curve $Ca_2MgSi_2O_7 : Ce^{3+}$ 0.4 mol% for different UV exposure with heating at 6.7°C/S.**

(b) TL glow curve of $Ca_2MgSi_2O_7 : Eu^{2+}$ 0.4 mol% for different UV exposure time with heating rate 6.7° C/S.

Sensitivity

Table 5 and fig. 6 gives a comparison of TL response of $Ca_2MgSi_2O_7 : Ce^{3+}$ 0.4 mol% phosphor with the other two phosphors. It is observed that the sensitivity of $Ca_2MgSi_2O_7$ phosphor is only 50% as that of standard one, when both were exposed to same dose of UV radiation.

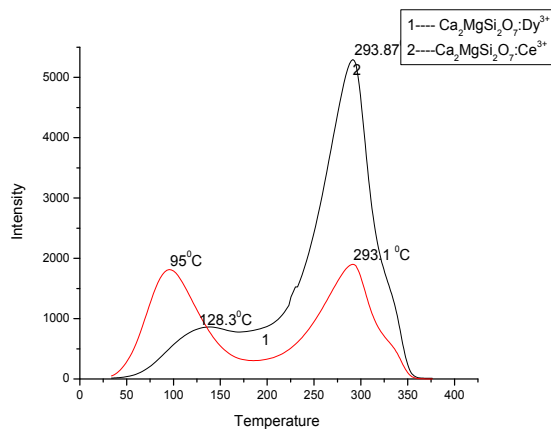**Fig. 6. Comparative TL glow curves of 0.4 mol% Ce^{3+} and Dy^{3+} doped $Ca_2MgSi_2O_7$ phosphor with fixed UV exposure time 5 min.**

Table 5: Comparison of TL response of Ce^{3+} and Dy^{3+} doped $Ca_2MgSi_2O_7$ phosphors.

Phosphors	Most intense TL peak temperature (°C)	Relative TL intensity
$Ca_2MgSi_2O_7 : Ce^{3+}$	293.87°C	5295.72
$Ca_2MgSi_2O_7 : Dy^{3+}$	293.1°C	3547.2

CONCLUSION

In conclusion a silicate compound $Ca_2MgSi_2O_7$ with different rare earth ions (RE = Ce, Dy) as well as different concentration (0.1 mol% , 0.2 mol% , 0.4 mol% & 0.5 mol%) were successfully synthesized by the solid state reaction and its luminescence properties were investigated. The examined TL glow curve gives the about kinetic parameters such as activation energy, frequency factor. All the kinetic parameters are calculated by initial rise method. All TL glow curves for different rare earth ions shows that intensity initially increases with rare earth concentration, approaches to an optimum values for 0.4 mol% of Ce^{3+}, Dy^{3+} and decreases with a further increase in rare earth ions concentration. The TL intensity of silicate compound $Ca_2MgSi_2O_7$ doped with rare earth Ce, Dy depends upon the UV exposure time and it were found to be maximum for 5min exposure time in Ce^{3+} and 10min exposure time in Dy^{3+} ion. From TL studies it is confirmed that Ce^{3+} doped $Ca_2MgSi_2O_7$ is a good material for dosimetry applications. From sensitivity of Ce^{3+} doped $Ca_2MgSi_2O_7$ is less than ($\approx$ 50%) as compared to other rare earth doped phosphor. It should be noted that the 293.87°C peak observed in $Ca_2MgSi_2O_7$: Ce can be used in high temperature dosimetry applications with more advantages. Because TL peak of standard one dosimetry material ($CaSO_4$: Dy) is about 230°C only.

ACKNOWLEDGEMENT

We are very thankful to Dr. D.P. Bisen for his valuable suggestion for sample preparation and investigation of luminescent properties.

REFERENCE

1. Lin, Y., Nan, C., Zhou, X., *et. al*, *J. Lumin.*. 94/95, V. **19** (2001)
2. Lin, Y., Tang, Z., Zhang, Z. and Nan, C .W., *J. Alloys Comp.*, **348**, 76 (2003).
3. Xi-Xian, L., Jin-xia, D., Guang–xu, L., *et. al.*, *Chinese J. Lumin*, **24**, 165 (2003).
4. Akiyama, Xu, M., Taria, C.M., Nonaka, M.K. and Watanabe, *Philosophical Magazine Letters*, **79**, 169, 735-740 (1999).
5. Brahme, N., Bisen, D.P., Kher, R.S. and Khokhar, M.S., *Phys. Procidea*, **2**, 431-440 (2009).
6. Chandra, B.P., *Pramana*, **19**, 455 (1983).
7. Kawano, Y., Woog Kim, S., Ishigaki, T., Takaba, H. and Sato, M., *Optical Materials Express*, **1770**, No. **9**, DOI : 10 1364.
8. Tamrakar, R.K., Bisen, D.P. and Brahme, N., *Research on Chemical Intermediates*, **40**, 1771-1779 (2014).
9. Wu, H., Hu, Y., Chen, L., Wang, X., *Mater. Lett.*, **65**, 2676–2679 (2011).
10. Y.C., Fu, Liu, B., Zhang, G., Chen, Y., Qi, Z. and Luo, X., *J. Lumin.,* **1,** 122–123 (2007).
11. Chen, R., Kirsh, Y., *Analysis of Thermally Stimulated Processes*, Pergamon Press (1981).